DOI: https://doi.org/10.14311/TPFM.2025.014

A STABLE SMOOTHED PARTICLE HYDRODYNAMICS SCHEME: APPLICATION ON FREE SURFACE FLOWS WITH OPEN BOUNDARIES

T. Halada [1,2], L. Beneš [2]

[1] **Centre of Hydraulic Research, Jana Sigmunda 313, 78349 Lutin, Czech Republic**

[2] **Department of technical mathematics , Faculty of Mechanical Engineering, Czech Technical University in Prague , Karlovo náměstí 13, 121 35 Praha, Czech Republic**

Abstract

In Smoothed Particle Hydrodynamics (SPH) method, dealing with free surface flows, artificial viscosity is frequently used to stabilize the computations. Artificial viscosity is associated with excessive dissipation. However, using only the physical viscosity, issues with stability arise. In fact, artificial viscosity hides some of the problems of a widely used SPH schemes. In order to resolve stability issues, we employed conservative modification of boundary integrals formulation of boundary conditions together with midpoint scheme to solve free surface flows in three-dimensional open geometries including open boundaries.

Keywords: free surface flows, SPH, boundary conditions

1 Introduction

In recent years, there has been significant progress in simulations of free surface flow problems. Leaving aside the progress in adaptive mesh techniques, which allow a sharp capture of interfaces, the main contribution is the use of mesh-free methods based on the Lagrangian description of the continuum, especially the Smoothed Particle Hydrodynamics (SPH) method [1, 2].

At present, the SPH method is becoming a widely used tool for modeling free surface flows. In SPH, the fluid is discretized by a finite number of constant-mass Lagrangian particles, and the motion of particles, which underlie the governing equations, provides information about how the fluid evolves. Due to the Lagrangian nature, the free surface is automatically captured [13].

To deal with the phenomena of free surface flow, SPH - in most of its applications - works with some kind of weakly compressible model of fluid. Although there are truly incompressible (or divergence-free) formulations of the method [3], the weakly compressible formulation (WCSPH) allows us to construct explicit schemes, resulting in algorithms suitable for massively parallel computing using modern architectures, particularly graphics cards (GPUs) [4, 5].

In order to improve the stability of the weakly compressible model SPH in its pure Lagrangian form, first artificial viscosity was included to suppress velocity oscillations [6] and later the artificial diffusive term was included to resolve spurious pressure oscillations resulting in the so-called δ-WCSPH formulation [7].

In this work, we deal with the simulation of free surface flow with open boundaries in a complex three-dimensional geometry of the discharge object of the pump station. Problems of this kind are suitable for the SPH method, although discretizing complex geometries with narrow sections and dealing with inflow and outflow boundary conditions, especially in case of back pressure, are still not straightforward. Similar cases have been successfully solved with the $\delta-$WCSPH formulation, including artificial viscosity. However, artificial viscosity is known to be excessively dissipative [6]. Here we aim to solve this problem using a model of a viscous fluid considering only the physical viscous term. As it turns out, by omitting the artificial viscosity, stability problems appear in this case, which needs to be addressed by revisiting the used scheme.

As a representative of these problems, we used a laboratory model of v-shaped overflow with previously experimentally measured water levels [8]. First, originating from the widely used $\delta-$WCSPH scheme with boundary integrals formulation of boundary conditions (the input geometry makes multilayer variants difficult to use), then we sketch its problems and modify the discretization. Afterwards, comments on time integration are made followed by the obtained results. All the schemes, problems, and results mentioned were implemented and are available in the open source SPH code TNL-SPH [9] developed by the authors under the TNL library [10].

2 Physical model and SPH scheme

To solve water free surface flows, most of the WCSPH applications assume inviscid weakly compressible barotropic fluid in isothemal flow. Weak compressibility means that the variations of density up to one percent from the reference value are allowed. The relation between density and pressure is given by the Cole equation of state [11], which has proven useful for these types of problem [13]. The weakly compressible assumption is controlled by the numerical speed of sound c_s.

We use $\langle\bullet\rangle = \langle\bullet\rangle^{\Omega} + \langle\bullet\rangle^{\partial\Omega}$ to denote the SPH approximation, which consists of the approximation inside the domain Ω and near the boundary $\partial\Omega$ (including the way we resolve the boundary conditions) [2]. In our case, we realize boundary conditions by boundary integrals formulation (BI) [12], which discretizes the boundary using a single layer of boundary particles or elements. Discretizing the fluid using particles with initial spacing Δx and constant mass $m = \rho_0(\Delta x)^n$, where n is the dimension of the problem, the governing equations in Lagrangian form are rewritten in terms of ordinary differential equations for individual particles

$$\frac{\mathrm{D}\mathbf{x}_i(t)}{\mathrm{D}t} = \mathbf{v}_i(t) \tag{1a}$$

$$\left\langle \frac{\mathrm{D}\rho}{\mathrm{D}t} \right\rangle_i (t) = -\rho_i \left\langle \nabla\cdot\mathbf{v} \right\rangle_i (t) + \mathcal{D}_i^{\delta}(t) \tag{1b}$$

$$\left\langle \frac{\mathrm{D}\mathbf{v}}{\mathrm{D}t} \right\rangle_i (t) = -\frac{1}{\rho_i(t)}\langle\nabla p\rangle_i(t) + \mathcal{V}_i^{\alpha}(t) - \mathbf{g} \tag{1c}$$

$$p_i(t) = \frac{c_s^2\rho_0}{\kappa}\left[\left(\frac{\rho_i(t)}{\rho_0}\right)^{\kappa} - 1\right] \tag{1d}$$

where $\mathrm{D}(\bullet)/\mathrm{D}t$ denotes material derivatives, index i is used to denote individual particles, $\mathbf{x}, \mathbf{v}, \rho, p$ represent particle position, velocity, density and pressure respectively, c_s is the numerical speed of sound, ρ_0 is the referential density, $\kappa = 7$ is the Poisson constant, $\mathbf{g}$ represents gravity, $\mathcal{D}_i^{\delta}$ stands for artificial diffusive term included in order to suppress spurious pressure oscillations and $\mathcal{V}_i^{\alpha}$ denotes artificial viscosity [6]. The operators are given as $\langle\nabla\cdot\mathbf{v}\rangle_i = \langle\nabla\cdot\mathbf{v}\rangle_i^{\Omega,\mathrm{asym.}} + \langle\nabla\cdot\mathbf{v}\rangle_i^{\partial\Omega,\mathrm{asym.}}$, the pressure gradient is discretized as $\langle\nabla p\rangle_i = \langle\nabla p\rangle_i^{\Omega,\mathrm{sym.}} + \langle\nabla p\rangle_i^{\partial\Omega,\mathrm{sym.}}$. Discretisation of individual operators takes form

$$\langle\nabla\cdot\mathbf{v}\rangle_i^{\Omega,\mathrm{asym.}} = \sum_{j\in\mathcal{F}}(\mathbf{v}_j - \mathbf{v}_i)\nabla_i W_{ij}^{\mathcal{L}} V_j, \qquad \langle\nabla\cdot\mathbf{v}\rangle^{\partial\Omega,\mathrm{asym.}} = \sum_{j\in\mathcal{B}}(\mathbf{v}_j - \mathbf{v}_i)\,\mathbf{n}_j W_{ij}^{\mathcal{L}} S_j \tag{2}$$

$$\langle\nabla p\rangle^{\Omega,\mathrm{sym.}} = \sum_{j\in\mathcal{F}}(p_i + p_j)\nabla_i W_{ij}^{\mathcal{L}} V_j, \qquad \langle\nabla p\rangle^{\partial\Omega,\mathrm{sym.}} = \sum_{j\in\mathcal{B}}(p_i + p_j)\mathbf{n}_j W_{ij}^{\mathcal{L}} S_j \tag{3}$$

where the indices i, j denotes individual particles, $W_{ij}^{\mathcal{L}} = \mathcal{L}(\mathbf{x}_i)W_{ij}$ where $W_{ij} = W(\mathbf{x}_i - \mathbf{x}_j, h)$ is the smoothing function, h stands for the smoothing length and $\mathcal{L}(\mathbf{x}_i)$ is smoothing function correction, $V_j = m/\rho_j$ is the particle volume, $\mathbf{n}_j$ and S_j denotes boundary normal and size of boundary particle (element) and $\mathcal{F}$ and $\mathcal{B}$ denotes set of fluid and boundary particles. For the smoothing function correction we assume $\mathcal{L}(\mathbf{x}_i) = 1/\langle\gamma\rangle_i$, where $\langle\gamma\rangle_i = \sum_{j\in\mathcal{F}} W_{ij}V_j$ is approximation of Shepard factor.

Assuming diffusive term proposed by Molteni [7], the artificial diffusion controlled by parameter δ (with usual value $\delta = 0.1$) is given by

$$\mathcal{D}_i^{\delta} = 2\delta h c_s \sum_{j\in\mathcal{F}}(\rho_j - \rho_i)\,\frac{(\mathbf{x}_i - \mathbf{x}_j)\cdot\nabla_i W_{ij}^{\mathcal{L}}}{\|\mathbf{x}_i - \mathbf{x}_j\|^2} V_j \tag{4}$$

and artificial viscosity controlled by parameter α (with usual value from interval $\alpha \in [0.01, 0.1]$) takes form

$$\mathcal{V}_i^{\alpha} = \begin{cases} 2\alpha h c_s \displaystyle\sum_{j\in\mathcal{F}} \frac{\rho_i\rho_j\pi_{ij}}{(\rho_i + \rho_j)}\nabla_i W_{ij}^{\mathcal{L}} V_j & (\mathbf{v}_i - \mathbf{v}_j)\cdot(\mathbf{x}_i - \mathbf{x}_j) < 0 \\ 0 & (\mathbf{v}_i - \mathbf{v}_j)\cdot(\mathbf{x}_i - \mathbf{x}_j) \geq 0 \end{cases}, \qquad \pi_{ij} = \frac{(\mathbf{v}_i - \mathbf{v}_j)\cdot(\mathbf{x}_i - \mathbf{x}_j)}{\|(\mathbf{x}_i - \mathbf{x}_j)\|^2}. \tag{5}$$

This formulation is one of the most used approaches to solving free surface flows and is implemented in numerous solvers.

Artificial viscosity has received much attention over the years, including revisiting its connection to physical viscosity [15]. By analyzing the term in the case that $(\mathbf{v}_i - \mathbf{v}_j) \cdot (\mathbf{x}_i - \mathbf{x}_j) < 0$, Laplacian of velocity is recovered. Nevertheless, since the effective viscosity depends on the smoothing length h, the term has a purely numerical effect and, as we can see in the limit $h \to 0$, we are solving an inviscid system. This is something that deserves attention because in this case, we cannot prescribe zero velocity for the boundaries (hoping for a non-trivial solution), otherwise the problem is ill-posed. However, this is something that is frequently done, see for example, [4, 14] and related works.

2.1 Including viscosity

To include viscosity we assume compressible Newtonian barotroic fluid in isothermal flow, with the Cole equation of state to link pressure and density which together with the artificial speed of sound enforces the weakly compressible behavior. Therefore, we need to replace the artificial viscosity in equation (1c) by discretization of the viscous forces $\mu\langle\Delta\mathbf{v} + 2\nabla(\nabla \cdot \mathbf{v})\rangle$.

As demonstrated in [16] the use of a no-slip boundary condition using boundary integrals requires an additional treatment of the boundary term since the presence of boundary normal $\mathbf{n}$ in the boundary integral formulas erases the contribution of wall shear stress.

Using Monaghan-Gingold [17] discretization of viscous term with addition first order expansion in the boundary interaction component to include effects in tangential direction, we end up with

$$\langle\Delta\mathbf{v} + 2\nabla(\nabla \cdot \mathbf{v})\rangle_i^{\Omega} = 2(n+2)\mu \sum_{j \in \mathcal{F}} \frac{(\mathbf{v}_i - \mathbf{v}_j) \cdot (\mathbf{x}_i - \mathbf{x}_j)}{\|(\mathbf{x}_i - \mathbf{x}_j)\|^2} \nabla_i W_{ij}^{\mathcal{L}} V_j \tag{6}$$

$$\langle\Delta\mathbf{v} + 2\nabla(\nabla \cdot \mathbf{v})\rangle_i^{\partial\Omega} = 2(n+2) \sum_{j \in \mathcal{B}} \frac{(\mathbf{v}_i - \mathbf{v}_j)}{(\mathbf{x}_i - \mathbf{x}_j) \cdot \mathbf{n}_j} W_{ij}^{\mathcal{L}} S_j. \tag{7}$$

However, using (6) and (7) instead of artificial in the system of equations (1c), problems arise with the stability of the simulations. The simulations diverge at some point. In fact, artificial viscosity, due to its excessive dissipation, hides several problems of the scheme.

The first thing to check is whether the discretized scheme conserves energy. For simplicity, assume that $\mathcal{L}(\mathbf{x}_i) = 1$ so $W_{ij}^{\mathcal{L}}$ reduces to W_{ij}. Following [18, 19], the instantaneous power balance of kinetic power depending only on the spatial discretization can be defined as

$$\langle P_k \rangle(t) = \sum_{i \in \mathcal{F}} m_i \mathbf{v}_i \cdot \left\langle \frac{\mathrm{d}\mathbf{v}}{\mathrm{d}t} \right\rangle_i (t). \tag{8}$$

Substituting for $\langle \mathrm{D}\mathbf{v}/\mathrm{D}t \rangle_i (t)$, the power power balance at particular time t can be split and rearranged

$$\langle P_k \rangle(t) + P_p(t) + \langle P_c \rangle(t) = \langle P_\mu \rangle(t) + (k-2)\langle P_{\nabla\gamma} \rangle(t) - \langle P \rangle^{\partial\Omega}(t) \tag{9}$$

where $P_p(t)$ is power due to external forces, $\langle P_c \rangle(t)$ is power connected with compressibility and $\langle P_\mu \rangle(t)$ is power of viscous forces. The term $\langle P_{\nabla\gamma} \rangle(t)$ was added to the power balance in [18] as a consequence of the discretization of the pressure gradient and presents a violation of energy conservation. Using the symmetric approximation (3) corresponds to $k = 2$, so the term cancels out. Another violation of energy conservation results from the realization of boundary conditions using the BI formulation. This is demonstrated for example in [20] and finally expressed in [19]

$$\langle P \rangle^{\partial\Omega} = \sum_{i \in \mathcal{F}} \sum_{j \in \mathcal{B}} (p_j \mathbf{v}_i + p_i \mathbf{v}_j) \cdot n_j W_{ij} V_i S_j. \tag{10}$$

As proposed in [19], the boundary term $\langle P \rangle^{\partial\Omega}$ can be canceled by prescribing the boundary values as $\mathbf{v}_j = -\mathbf{v}_i$ and $p_j = p_i$. This leads to following modified boundary integrals approximations

$$\langle \nabla \cdot \mathbf{v} \rangle_i^{\partial\Omega,\mathrm{conserv.}} = 2 \sum_{j \in \mathcal{B}} (\mathbf{v}_j - \mathbf{v}_i)\, \mathbf{n}_j W_{ij} S_j \tag{11}$$

$$\langle \nabla p \rangle_i^{\partial\Omega,\text{conserv.}} = 2p_i \sum_{j\in\mathcal{B}} \mathbf{n}_j W_{ij} S_j. \tag{12}$$

In an effort to improve energy conservation, we also omit the normalization by the Shepard factor $\langle\gamma\rangle_i$ (that is $\mathcal{L}(\mathbf{x}_i) = 1$ and $W_{ij}^{\mathcal{L}} = W_{ij}$) used in system (1), which breaks the symmetry of the interactions. Plugging all these parts together, we obtain resulting scheme

$$\frac{\mathrm{D}\mathbf{x}_i(t)}{\mathrm{D}t} = \mathbf{v}_i(t) \tag{13a}$$

$$\left\langle \frac{\mathrm{D}\rho}{\mathrm{D}t} \right\rangle_i (t) = -\rho_i \langle \nabla \cdot \mathbf{v} \rangle_i (t) + \mathcal{D}_i^{\delta} \tag{13b}$$

$$\left\langle \frac{\mathrm{D}\mathbf{v}}{\mathrm{D}t} \right\rangle_i (t) = -\frac{1}{\rho_i(t)} \langle \nabla p \rangle_i(t) + \mu \langle \Delta \mathbf{v} + 2\nabla (\nabla \cdot \mathbf{v}) \rangle - \mathbf{g} \tag{13c}$$

$$p = \frac{c_0^2 \rho_0}{\gamma} \left[\left(\frac{\rho}{\rho_0} \right)^{\gamma} - 1 \right] \tag{13d}$$

where the divergence of velocity is discretized as $\langle \nabla \cdot \mathbf{v} \rangle_i = \langle \nabla \cdot \mathbf{v} \rangle_i^{\Omega,\text{asym.}} + \langle \nabla \cdot \mathbf{v} \rangle_i^{\partial\Omega,\text{conserv.}}$, the pressure gradient is discretized as $\langle \nabla p \rangle_i = \langle \nabla p \rangle_i^{\Omega,\text{sym.}} + \langle \nabla p \rangle_i^{\partial\Omega,\text{conserv.}}$ and the viscos forces are discretized by $\langle \Delta \mathbf{v} + 2\nabla (\nabla \cdot \mathbf{v}) \rangle = \langle \Delta \mathbf{v} + 2\nabla (\nabla \cdot \mathbf{v}) \rangle^{\Omega,\text{MG}} + \langle \Delta \mathbf{v} + 2\nabla (\nabla \cdot \mathbf{v}) \rangle^{\partial\Omega,\text{MG,no-slip}}$.

2.2 Time integration scheme

The last missing part is the time integration scheme. Originally, we have considered the widely used Verlet scheme [21] and the symplectic position Verlet scheme [22]. Using conservative boundary conditions and integrating the system (13) using the Verlet scheme, we were able to solve some of the considered configurations of the problems described below which were not stable with the original BI formulation without artificial viscosity. However, the Verlet scheme includes intermediate steps employed in every m-th integration step using explicit Euler integration, which includes additional dissipation. Most of the considered setups (with small tweaks in geometry or inlet boundary conditions with respect to the presented settings) still remain unstable regardless of our effort to adjust the CFL and time step.

In order to resolve stability issues, we employed the semi-implicit midpoint scheme, which is unconditionally stable.

$$\hat{\rho}_i^m(t_{n+1/2}) = \rho_i^n + \frac{\Delta t}{2} \widetilde{\rho}_i^m, \qquad \widetilde{\rho}_i^{m+1} = f^m \left\langle \frac{\mathrm{D}\rho}{\mathrm{D}t} \right\rangle_i (t_{n+1/2}) + (1 - f^m) \widetilde{\rho}_i^m \tag{14}$$

$$\hat{\mathbf{v}}_i^m(t_{n+1/2}) = \mathbf{v}_i^n + \frac{\Delta t}{2} \widetilde{\mathbf{v}}_i^m, \qquad \widetilde{\mathbf{v}}_i^{m+1} = f^m \left\langle \frac{\mathrm{D}\mathbf{v}_i}{\mathrm{D}t} \right\rangle_i (t_{n+1/2}) + (1 - f^m) \widetilde{\mathbf{v}}_i^m \tag{15}$$

where $f_m \in [0, 1]$ is relaxation. The iteration is controlled by residuals of the energy conservation

$$R_{\Delta t}[E](t) = \sum_{j\in\mathcal{F}} \left| m\mathbf{v}_i(t) \cdot \left(\left\langle \frac{\mathrm{D}\mathbf{v}}{\mathrm{D}t} \right\rangle_i (t) \right) \right| + \sum_{j\in\mathcal{F}} \left| \frac{m p_i(t)}{\rho_i^2(t)} \left(\left\langle \frac{\mathrm{D}\rho}{\mathrm{D}t} \right\rangle_i (t) \right) \right| \tag{16}$$

Following [18], relaxation is not considered at the beginning of each time step. The relaxation factor f_m increases linearly if the residuals decay slower than required. In that case $f_{m+1} = \Delta_f + (1 - \Delta_f) f_m$ where Δ_f is the selected increase in the relaxation coefficient.

To complete the description of the numerical algorithm, two additional procedures are employed. First, to ensure no-penetrable solid walls, in situations where a particle may move through the boundary, we use elastic bounce from the wall. Second, since every particle has assigned a certain volume, it cannot approach to close to the boundary, otherwise it would geometrically exceed the walls. To deal with this, after every corrector step we employ *near-boundary particle shifting technique*, to slightly adjust the particle positions.

We would like to highlight that the selection of integration scheme and introduction of conservative boundary approximations are complementary and both need to be considered in order to realize the simulations. The steps described above form a stable SPH scheme that is capable

of solving problems where the SPH approaches used so far fail. We also note that employing near-boundary particle shifting technique with different integration approaches then the midpoint led to the bow-up of the simulation. Last, we are not sure why variants with symplecitc position Verlet scheme fail, which is something that has yet to be analyzed.

3 Results

We simulated $t_{\text{phys.}} = 15$ s of physical time of the free surface flow in an open channel with v-shaped overflow, previously described in [8]. We start with empty channel, so the simulations include the run-up state. For the inlet, we prescribe a fixed flow rate $Q = 11.4$ ls^{-1}, using a constant velocity profile and a hydrostatic pressure profile. The hydrostatic pressure profile is updated according to the water level in the tank above the overflow. After approximately $t_{\text{phys.}} = 10$, the filling of the empty object reaches the pseudo-stationary state and the average water levels in the system do not change anymore. The water level in the outflow channel is set by using the outflow flood gate at $h_{\text{out}} = 0.095$ m. For the downstream outlet boundary, a zero gradient of velocity and pressure are prescribed. Inlet and outlet boundary conditions are realized using multi-layer buffers. In the inlet buffer, the particles are generated on the basis of minimal energy of the stable state, which reduces the spurious oscillations caused by the inlet.

As fluid we assume water with reference density $\rho_0 = 1000$ kgm^{-3} and dynamic viscosity $\mu = 0.000102$ Pas^{-1}. We assume an initial particle spacing $\Delta x = 0.003$ m, the smoothing length is given as $h = \sqrt{3}\Delta x$, for the smoothing function we use the Wendland C2 function. The numerical speed of sound is $c_s = 84$ ms^{-1}. To smooth the pressure fields, the diffusive term proposed by Molteni is used with $\delta = 0.1$.

For the midpoint scheme, we stop the iteration if the residual decays below $R_{\Delta t}[E](t_{n+1/2}) < 0.02$ or after 30 iteration steps. The minimal residual decay to modify the relaxation coefficient is $R^m_{\Delta t}[E](t_{n+1/2})/R^{m-1}_{\Delta t}[E](t_{n+1/2}) = 0.2$, with an increase in the relaxation coefficient $\Delta_f = 0.1$. We used the Courant number Co $= 0.5$ with an initial time step $\Delta t = 10^{-5}$ s.

The calculations were performed using open source TNL-SPH [9] code developed by the authors. All the presented simulations and setups can be found within the TNL-SPH project.

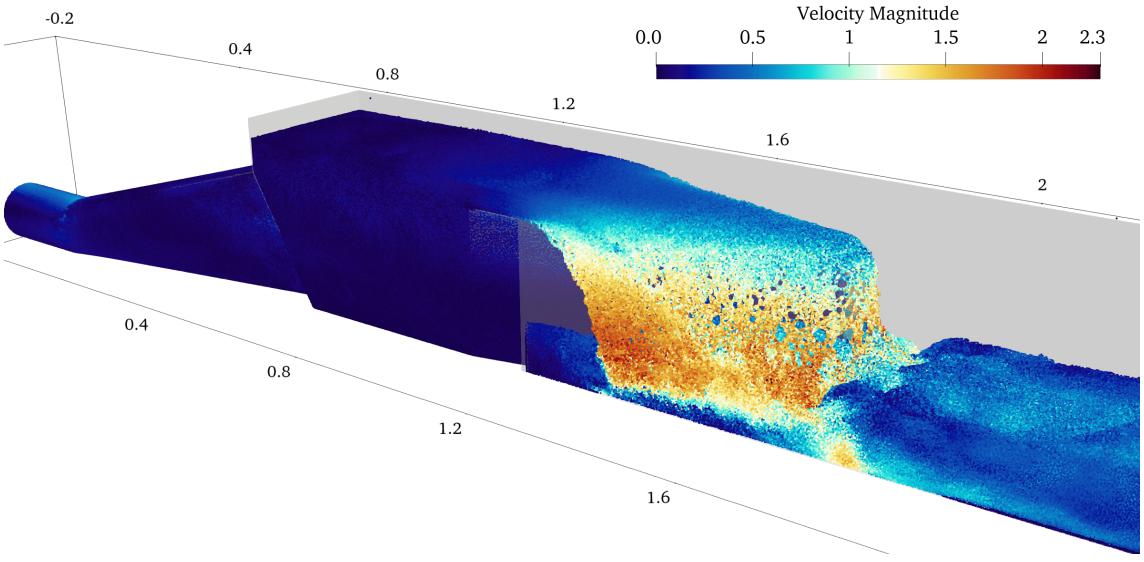

Figure 1: Simulation snapshot in fully developed state at $t = 15$ s, using the particle representation.

In Figure 2 we compare the average water levels obtained from the simulations with the experimental data previously measured by the Center of Hydraulic Research. To evaluate the water level at some point of the channel given by the $[x_0, y_0]$ coordinates (we assume that the geometry is oriented in such a way that the water level changes in the z-axis), we proceed from the bot-

tom of the channel (denoted z_0), moving in the z direction by steps Δx. In each of these points $\mathbf{x}_k = [x_0, y_0, z_0 + k\Delta x], k \in \mathbb{N}$, we evaluated the normalized particle concentration $\gamma(\mathbf{x}_k)$.

In the volume of the fluid, the support of the smoothing function is completely occupied by neighboring particles, and we have $\gamma(\mathbf{x}_k) \simeq 1$. As a surface, we take points $\mathbf{x}_k$ where $\gamma(\mathbf{x}_k) = 0.5$, which corresponds to roughly half filling of the weight function support. For averaging, we assume a time interval from $t = 10$ s to $t = 15$ s, taking a snapshot every $t_s = 0.1$ s.

The small variation in height for points just above the level in the outflow channel may be due to the way the level is detected. In these spots, the surface is very ragged and the criterion used to determine the level fails at a given resolution. The step-like structure of the water levels that is clearly visible in the figure 2 is caused by the lattice structure of the test points $\mathbf{x}_k$ where we evaluate the concentrations of particles..

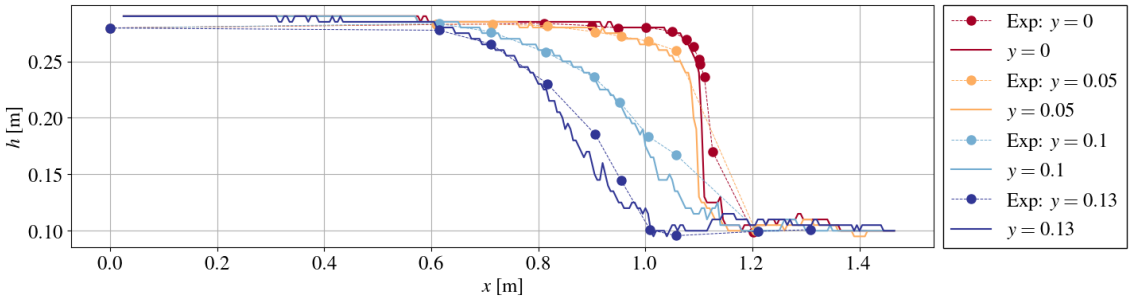

Figure 2: Averaged water levels in the central plane of the channel $y = 0$ m and planes at $y = 0.05$ m, $y = 0.1$ and water level at the wall $y = 0.13$. Simulation data *(solid lines)* are compared experimental data *(filled circles with thin dashed line)*.

We also note that the standard deviation of the experimental data is not provided. Taking into account the chaotic behavior of the free surface, we should keep this in mind when comparing the results.

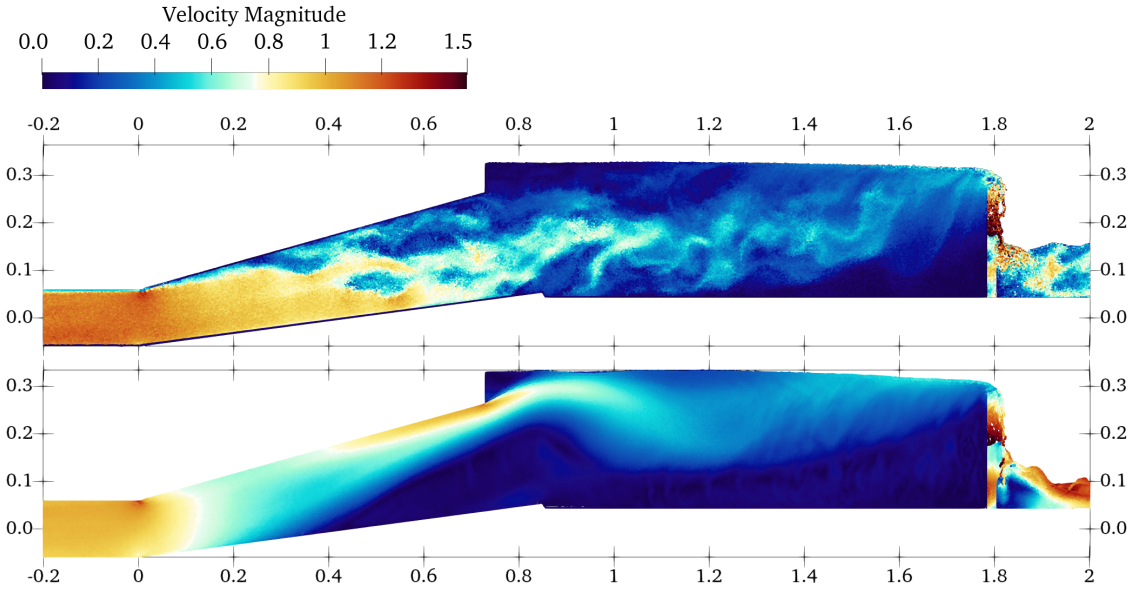

Figure 3: Snapshot of half-cut (in central plane) of the channel at $t = 15$ s in the particle representation showing the instantaneous velocity. *Top:* results obtained with scheme (13) using physical viscosity, *bottom:* results obtained with scheme (1) with artificial viscosity.

In figure 3, we compare the results obtained using the scheme (13) with the physical viscosity

at the top, with the results obtained using the original scheme (1) with the artificial viscosity at the bottom. The figure presents a snapshot of the instantaneous velocity field in the central cut of the channel at $t = 15$ s. For the artificial viscosity setup, we set $\alpha = 0.01$ which corresponds to the commonly used value. Solving the system (1), the boundary condition for the wall was adjusted according to the fact that we deal with an inviscid system to a zero normal velocity. Moreover, for the case with artificial viscosity, we integrated the system using the Verlet scheme.

For a detailed comparison of the two models, validation of the velocity field would also be required. Nevertheless, we decided to include this result in order to highlight the differences between the two models. At least informally, we can say that the velocity field obtained from the artificial viscosity model seems to deviate from the expected physical behavior. The water levels in both cases are almost similar.

4 Conclusion

In the presented work, we focused on numerical stability issues in simulations of free surface flows with open boundaries. Leaving aside standard SPH artificial viscosity and using only the physically corresponding viscous term, problems hidden by artificial viscosity excessive dissipation arise and the simulations start to be difficult to realize due to loss of stability. To address these problems, we employed semi-implicit midpoint time integration scheme, which on its own is not enough to resolve the issues. As was recently shown, spatial discretisation, especially the boundary integrals formulation of boundary conditions, needs to be revisited with respect to the energy conservation. This eventually results in an unconditionally stable scheme that is able to handle the target simulations. Although the semi-implicit time integration is used, in the current setup, it is necessary to take into account the technical restrictions on Δt associated mainly with the realization of inputs and outlets. In our work, we demonstrate that this approach is also promising for problems with open boundaries in complex geometries.

Finally, we note that, utilizing the conservation modification of boundary integrals formulation, in some cases we were even able to succeed even using the conventional Verlet time integration scheme. However, the used form of the Verlet scheme includes additional dissipation introducing intermediate explicit Euler integration step after every m-th integration step. Besides, one needs to pay much more attention to tuning boundary condition parameters (for example the elastic bounce factor) and the numerical parameters over all. For some configurations of the problem we were dealing with, using the Verlet scheme, we were unable to perform the simulations regardless of the time step decreasing.

We note that in cases where the explicit scheme worked, it was approximately twice faster than the semi-implicit midpoint scheme with current setup. Nevertheless, there is still room for improvement, and in the future work we would like to focus on improving the setup of midpoint scheme to reduce its computation time.

To conclude, we were able to simulate the free surface flow in the complex three-dimensional geometry of the discharge object, which includes open boundaries, using the SPH method, which works only with the physical viscosity. Simulations of this type have so far not been possible with existing SPH schemes due to numerical stability issues.

Acknowledgment

This research was supported by *Ministry of Education, Youth and Sports of the Czech Republic* under the project *CZ.02.01.01/00/23_021/0008954 "Hydrodynamic machines for smart energetics"*. Computational resources were provided by the *e-INFRA CZ project (ID:90254)*, supported by the *Ministry of Education, Youth and Sports of the Czech Republic.*

References

[1] Gingold, R. & Monaghan, J.: Smoothed particle hydrodynamics: theory and application to non-spherical stars.. *Monthly Notices Of The Royal Astronomical Society.* **181** pp. 375-389 (1977)

[2] Violeau, D.: Fluid mechanics and the SPH method: theory and applications. (Oxford University Press,2015)

[3] Shao, S. & Lo, E.: Incompressible SPH method for simulating Newtonian and non-Newtonian flows with a free surface. *Advances In Water Resources*. **26**, 787-800 (2003,7)

[4] Domínguez, J. et al.: DualSPHysics: from fluid dynamics to multiphysics problems. *Computational Particle Mechanics*. (2021)

[5] Cercos-Pita, J.: AQUAgpusph, a new free 3D SPH solver accelerated with OpenCL. *Comput Phys Commun*. (2015)

[6] Monaghan, J. & Pongracic, H.: Artificial viscosity for particle methods. *Applied Numerical Mathematics*. **1**, 187-194 (1985)

[7] Molteni, D. & Colagrossi, A.: A simple procedure to improve the pressure evaluation in hydrodynamic context using the SPH. *Comput Phys Commun*. **180** (2009)

[8] Sedlář, M., Machalka, J. & Komárek, M.: Modeling and Optimization of Multiphase Flow in Pump Station. *Journal Of Physics: Conference Series*. **1584**, 012070 (2020,7)

[9] Halada, T., Oberhuber, T. & Klinkovsky, J.: Template Numerical Library - TNL-SPH. *GitLab Repository*. (2024), https://gitlab.com/tnl-project/tnl-sph

[10] Oberhuber, T., Klinkovský, J. & Fučík, R.: TNL: NUMERICAL LIBRARY FOR MODERN PARALLEL ARCHITECTURES. *Acta Polytechnica*. **61**, 122-134 (2021)

[11] Cole, R. Underwater explosions. (Princeton Univ. Press, 1948)

[12] Macia, F., Gonzalez, L., Cercos-Pita, J. & Souto-Iglesias, A.: A Boundary Integral SPH Formulation: Consistency and Applications to ISPH and WCSPH. *Progress Of Theoretical Physics*. **128**, 439-462 (2012,9)

[13] Monaghan, J.: Simulating free surface flows with SPH. *J Comput Phys*. **110** (1994)

[14] English, A. et al.: Modified dynamic boundary conditions (mDBC) for general-purpose smoothed particle hydrodynamics (SPH): application to tank sloshing, dam break and fish pass problems. *Computational Particle Mechanics*. (2021,4)

[15] Colagrossi, A., Durante, D., Bonet Avalos, J. & Souto-Iglesias, A.: Discussion of Stokes' hypothesis through the smoothed particle hydrodynamics model. *Physical Review E*. **96** (2017,8)

[16] Němeček, J., Halada, T. & Beneš, L. Analysis of Boundary Conditions Properties in the SPH Method. *Topical Problems Of Fluid Mechanics 2024*. pp. 150-157 (2024)

[17] Monaghan, J. & Gingold, R.: Shock simulation by the particle method SPH. *Journal Of Computational Physics*. **52**, 374-389 (1983,11), http://dx.doi.org/10.1016/0021-9991(83)90036-0

[18] Cercos-Pita, J., Merino-Alonso, P., Calderon-Sanchez, J. & Duque, D.: The role of time integration in energy conservation in Smoothed Particle Hydrodynamics fluid dynamics simulations. *European Journal Of Mechanics - B/Fluids*. **97** pp. 78-92 (2023,1)

[19] Cercos-Pita, J., Duque, D., Merino-Alonso, P. & Calderon-Sanchez, J.: Boundary conditions for SPH through energy conservation. *Computers & Fluids*. **285** pp. 106454 (2024,12)

[20] Halada, T. & Beneš, L.: Effect of boundary conditions on particle spurious movement in Smoothed Particle Hydrodynamics method. *Journal Of Computational And Applied Mathematics*. **427** pp. 115133 (2023,8)

[21] Verlet L.: Computer experiments on classical fluids. I. Thermodynamical properties of Lennard-Jones molecules. *Physical Review*, **159**, pp. 98-103 (1967)

[22] Leimkuhler B. J. & Matthews C.: Molecular Dynamics. Springer International PU, (2016)